Fused Filament Fabrication of Dynamically Crosslinked Network Derived from Commodity Thermoplastics

Goutam Prasanna Kar, Xueyan Lin, Eugene Michael Terentjev *

Cavendish Laboratory, University of Cambridge, JJ Thomson Avenue, Cambridge CB3 0HE, U.K.

*Email: emt1000@cam.ac.uk

Abstract: Massive carbon footprint is associated with ubiquitous use of plastics and their afterlife. Greenhouse gas (GHG) emission of plastics is rising and increasingly consuming the global "carbon budget". It is, hence, paramount to implement an effective strategy to reclaim post-consumer plastic as feedstock for technologically innovative materials. Credible opportunity is offered by advances in materials chemistry and catalysis. Here we demonstrate that by dynamically crosslinking thermoplastic polyolefins, commodity plastics can be upcycled into technically superior and economically competitive materials. A broadly applicable crosslinking strategy has been applied to polymer containing solely carbon-carbon and carbon-hydrogen bonds, initially by maleic anhydride functionalization, followed by epoxy-anhydride curing. These dynamic networks show a distinct rubber modulus above the melting transition. We demonstrate that sustainability and performance do not have to be mutually exclusive. The dynamic network can be extruded into a continuous filament, to be in 3D printing of complex objects, which retain mechanical integrity of the vitrimer. Being covalently crosslinked, these networks show thermally triggered shape memory response, with 90% recovery of a programmed shape. This study opens a possibility of reclaiming recycled thermoplastics through imparting performance, sustainability and technological advances on the re-processed plastic.

KEYWORDS: additive manufacturing, shape memory polymers, epoxy-anhydride crosslinking, dynamic covalent chemistry, vitrimer, thermoplastic recycling

Introduction

Fossil fuel-based feedstock are the building blocks of majority of plastics today.[1] Since last four decades plastics production has quadrupled. Ever increasing anthropogenic GHG emission is associated with proliferating plastics production, endangering environment. Global life-cycle GHG emission of plastic were 1.7 of Gt of CO_2-equivalent (CO_2e) in 2015 and projected to reach 6.5 Gt CO_2e by 2050. It is estimated that if the current trend in GHG emission from plastics is continued it will consume 15% of global 'carbon budget' by 2050, thus presenting a critical concern to global effort to curb total anthropogenic carbon emission.[2]

Production of carbon-intensive virgin polymers can be significantly reduced by recycling after the service life of commodity plastics.[3] Globally, over 150 million tons of plastic are disposed annually and only about 10% are being recycled. Megatons of this plastic can be an untapped resource and a valuable feedstock.[4] Conventional mechanical recycling is a downward spiral in terms technical and monetary values, caused by deteriorating mechanical properties due to the incomplete purification. Energy recovery as an end-of-life treatment such as incineration leads to release of toxins and carbon emission. It is thus paramount to develop an efficient strategy to enable polymers to remain inherently recyclable without compromising their material properties. In principle, it is possible to chemically tailor functionality of polymer backbone to remake high valued materials with minimal loss of performance, thus enable re-entry into functional life-cycle – such a feat is the hallmark of cradle-to-cradle life cycle of plastics having profound impact in mitigating GHG emission.[5, 6]

Canonically, synthetic polymers are classified into two distinct families - thermoplastics and thermosets. Held together by physical intermolecular forces, thermoplastics are simply entangled polymer chains, although lightweight, tough and reprocessable, they are often soluble, and cannot preserve mechanical integrity at elevated temperature. Thermosets, on the other hand, are covalently crosslinked networks, and thus tough, insoluble and withstand high temperature. However, being permanently crosslinked, these materials are 'petrified' after synthesis and, hence, cannot be reprocessed and repurposed. The fixed geometry of injection-molding restricts these high-performing thermoset materials to a limited set of shapes; they cannot be recycled and face detrimental end-of-life treatment such as incineration.[3]

Recent renaissance in thermoset chemistry has challenged this dogma by underpinning a molecular mechanism of bond exchange, leading to a characteristic elastic-plastic transition enabled by dynamic crosslinking. Dynamic covalent chemistry has been applied to fundamentally alter the viscoelastic behavior of thermosets.[7-9] When the covalent bond exchange is triggered by external stimuli, the crosslinks rearrange among themselves, facilitating plastic flow under stress (which is a very different process from the viscous flow of a melt). In the absence of trigger, the dynamic network behaves as a traditional thermoset. Several bond exchange reactions have been explored to impart dynamic nature in polymer network, such as transesterification[10], trasamidation of vinylogous urethanes[11],

olefin metathesis[12], disulfide metathesis[13], dioxaborolane metathesis[14, 15], thiol-disulphide exchange[16], transalkylation[17]. While the viscosity of thermoplastics is governed by monomer friction, the rate of bond exchange in the dynamically crosslinked network dictates the rate of its plastic flow at elevated temperature. The Arrhenius thermally-activated dependence of this rate enables reprocessing these materials like vitreous silica, hence these types of materials were named *vitrimers* by Leibler and co-workers.[18] This bridging of the thermo-mechanical behaviour between thermoplastics and thermosets results a breadth of smart materials. Advanced polymer characteristics, such as strong welding[19], shape memory response[20-22], and self-healing[13, 16, 23] has been demonstrated with first-generation thermoplastic vitrimers of different kinds. Given the intensive ongoing research, it is expected for dynamic covalent chemistry to produce a large library of smart materials enabling multitude of current application in aerospace, automobile, biomedical, flexible electronics, and other industrial fields.

Here we demonstrate a broadly applicable strategy of dynamic crosslinking in polymers containing solely carbon-carbon and carbon-hydrogen bonds. Thermoplastic polyolefin (TPO) such as polypropylene (PP) and polyethylene (PE), comprising C-C backbone constitute 75% of polymer produced globally.[1, 14] The absence of any functional groups in TPO makes them chemically inert, also making functionalization difficult. To address this challenge, Leibler et al.[14] have formed TPO-based vitrimers crosslinked by dioxaborolane; this approach was repeated in more recent work of Yang et al.[24] and Maaz et al.[25] However, the borolane bond exchange has a very low activation energy, and the resulting materials would creep at high temperature. Exploring other crosslinking options, He et al. used the imine bond exchange with activation energy ca. 57 kJ/mol,[26] while Saed et al. used the thiol-thioester bond exchange with activation ca. 110 kJ/mol[27]. In an attempt to form a vitrimer with an even higher thermal stability, we have used the di-epoxy crosslinking of functionalized TPO, looking for a higher activation energy of transesterification bond exchange, reported as ca.124 kJ/mol.[10]

Here, we continue to work with PP as a model system, and functionalize it by grafting the maleic anhydride (MA), to enable the robust epoxy-ester bonding. To help with transesterification, we now select a di-epoxy oligomer with an added hydroxyl group to demonstrate the production of a dynamic network and remarkable changes in its mechanical response to thermal stimulus.

Transformation of commodity thermoplastics into smart polymer materials can only be viable if the method is compatible with the current settings of polymer processing industry. In this context, a solvent-free melt compounder has been employed. Over the years, melt compounders have emerged in various forms that have been coupled to other post-processing steps, such as melt blowing and injection moulding. Additive manufacturing has added another dimension to materials design,[24] when functional polymeric materials are extruded as a continuous filament from a melt compounder, and then served to a 3D printer in the Fused Filament Fabrication (FFF) mode to produce digitally encoded structure on demand.[28, 29] Here, to demonstrate this process, the vitrimer derived from commodity plastics was manufactured into complex objects with high dimensional precession. After that, we verify that the material properties are preserved after FFF 3D printing process. This workflow will have an impact on producing technically innovative and economically competitive materials from a generic commodity plastic feedstock - a key milestone towards the reduction of GHG emission of plastics and the increase of their multiple use. Thermoplastics can also be 3D-printed, but vitrimers have a strong welding capacity to allow subsequent assembly of 3D printed parts – a property not available to thermoplastics. Being covalently crosslinked, semicrystalline plastic vitrimers will also possess a very strong shape memory response, which we particularly explore in this work.

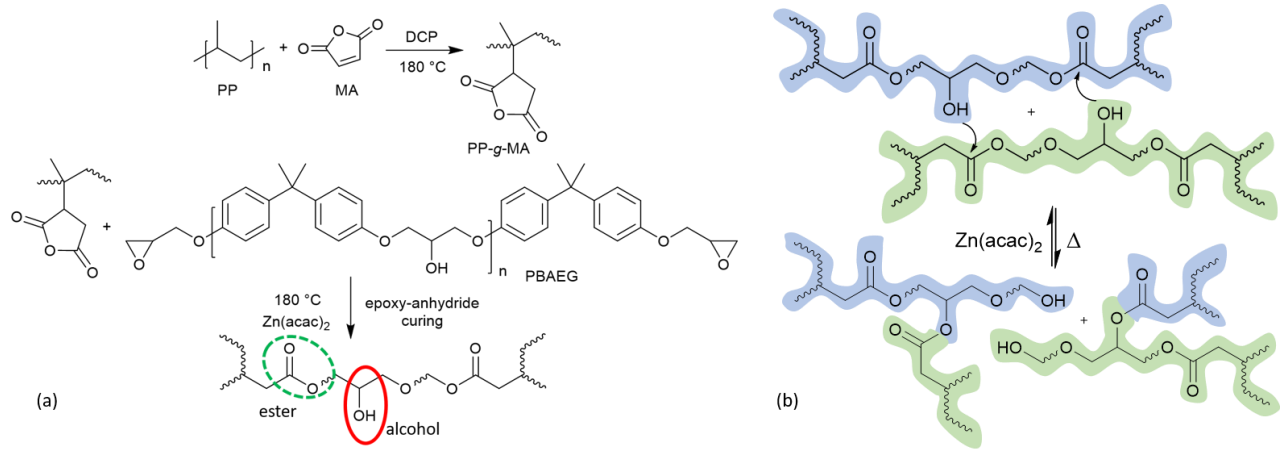

Figure 1. Synthesis of dynamically crosslinked PP network. (a) Two step functionalization of PP to introduce dynamic crosslinking: in the first step, anhydride functional groups are grafted onto PP backbone through free-radical reaction. $Zn(acac)_2$ catalyzed epoxy-anhydride curing is performed in the second step. (b) Thermally activated bond exchange between ester and alcohol functional groups (transesterification) in the dynamic network.

EXPERIMENTAL SECTION

Materials. Polypropylene (PP) with melt flow index 34 g/10 min was procured from INEOS Olefins & Polymers USA. Maleic anhydride (MA), dicumyl peroxide (DCP), poly(bisphenol A-co-epichlorohydrin) glycidyl end-capped (PBAEG) with M_n ≈1,075, zinc acetylacetonate hydrate ($Zn(acac)_2$), and xylene solvent were supplied by Sigma Aldrich (Merck).

Reactive extrusion. Dynamically crosslinked polyolefin network was synthesized through reactive extrusion in a laboratory scale twin screw extruder (HAAKE MiniLab 3, ThermoFisher) equipped with a recirculation channel. The whole process was carried out at 180 °C, with the screw speed of 100 rpm under N_2 flow. First, the required amount (4-5 g) of stock thermoplastic, MA (5 wt%) and the DCP (0.1 wt%) initiator were feed with the aid of a pneumatic press. After 10 min of circulation, we have verified the saturation of MA-grafting, and the di-functional epoxy crosslinking PBAEG, with $Zn(acac)_2$ (2.0 wt%) catalyst[30] were added into the extruder. After another 10 minutes, i.e. with the total residence time of 20-22 min, the crosslinked network was extruded. The resulting vitrimer was post-processed with a laboratory injection moulding (MiniJet, ThermoFisher), at 210 °C to obtain specimen with required dimensions. The uniform FFF filament with a diameter c.a. 1.75 mm was prepared by directly extruding the vitrimer through a custom-made nozzle with a diameter 2 mm. The scheme of the reactions is given in Figure 1.

Gel fraction. Samples of crosslinked vitrimer (weight = W_i) were immersed in xylene at 120 °C for 24 hours, with frequently changing solvent. The residual solid was dried at 120 °C under vacuum oven (typically for 6 h) till a constant weight (W_f) was achieved. Gel fraction (%) is measured as (W_f/W_i) × 100.

Melt flow index. An essential rheological characteristic of plastics is their melt flow index (MFI), which determines the regime and parameters of processing flow. The ASTM D1238 protocol describes the MFI measurement, which we have followed in this work. The PP and its derivatives falls into a category that is tested at 230 °C under the driving pressure of ΔP=0.3 MPa (achieved by supplying 2.16 kg load across the 9.5 mm cylinder bore). The plastic flow is measured through a standard die of d=2 mm diameter and L=8 mm length, the resulting MFI measured in units of grams per 10 min. Assuming Poiseuille flow, the volumetric flow rate Q is given by the expression

$$Q = \frac{\pi d^4}{128\,\eta L}\Delta P,$$

where η is the flow viscosity. Therefore, measuring the MFI in units of mass per unit time is equivalent to measuring the viscosity η of the flowing polymer.

FT-IR. MA grafting onto PP was confirmed by FT-IR. Compression moulded specimen was characterized by PerkinElmer Spectrum 100 FT-IR spectrometer in ATR mode as shown in Figure 2.

Titration. Percent MA-grafting was quantified by titration. Typically, 0.5 g MA-g-PP was dissolved in 50 ml xylene at 120 °C. Few drops of water was added into the mixture. Water hydrolyses maleic anhydride into carboxylic acid group that was titrated by alcoholic KOH (0.1 N) using 1 wt% bromothymol blue (in dimethyl formamide) as indicator. As the indicator added in the mixture (acidic solution) it appears as yellowish. Titration end point was identified by the appearance of faint blue colour. The amount of KOH (0.1 N) was noted, and the titration was performed in triplicate. The percent grafting was estimated by the relation as,

$f = (\text{ml KOH} \times N \times M_m)/ (2 \times 10)$,

where the normality, N = 0.1, and M_m = 100 is the molecular weight of grafted MA residue.

Differential scanning calorimetry (DSC). Melting (T_m) and crystallization (T_c) transition of the polymers were observed through DSC4000 from PerkinElmer. Typically, 5-10 mg of dried polymer were heated to 220 °C and kept isothermally for 5 min to erase the thermal history of the specimen. It was then cooled to 50 °C. T_c was observed in this cooling step. A subsequent re-heating to 220 °C reveals the T_m, see Figure 3. All the heating and cooling cycle was performed at 10 °C/min under N_2 flow. The percent crystallinity (χ_c) was calculated as,[31]

$$\chi_c = \frac{\Delta H_m}{\Delta H_m^0} \times 100\,,$$

Where, ΔH_m is heat of fusion of the polymer calculated from the area under the melting endotherm (2nd heating) and ΔH_m^0 is the standard heat of fusion of theoretically calculated 100 % crystalline polymer. ΔH_m^0 for PP is 209 J/g.[32]

Tensile testing (stress-strain). Room temperature stress-strain behaver were observed on Tinius Olsen 1ST universal testing machine mounted with a 2kN cell, with a fixed crosshead speed of 5 mm/min. ASTM D638 injection mould was used to prepare tensile specimen, see Figure 4(a).

Dynamic-mechanical analysis (DMA). Thermomechanical properties were measured by DMA 850 (TA Instruments). Prior to the test the samples were kept under vacuum for 5 h at 100 °C. For the measurement of temperature dependent dynamic modulus rectangular specimen of dimension ≈ 15 mm × 5 mm × 0.9 was placed between the clamps of DMA in tensile mode and equilibrated at 50 °C before starting the experiment. Evolution of dynamic modulus was observed at a constant frequency of 1 Hz, with 0.01 % strain, in the temperature range 50 - 240 °C with heating rate of 3 °C min^{-1}. A much slower heating rate of 0.5 °C min^{-1} was also examined to observe the equilibrium melting transition, (see Figure 5(a)).

'Iso-stress' creep testing. The plastic flow (creep) behaviour of dynamically crosslinked network was observed beyond the melting transition. Rectangular specimen was placed in the DMA clamps in tensile mode and equilibrated at the probe temperature for 5 min. An instantaneous stress of 20 kPa was applied and was kept constant

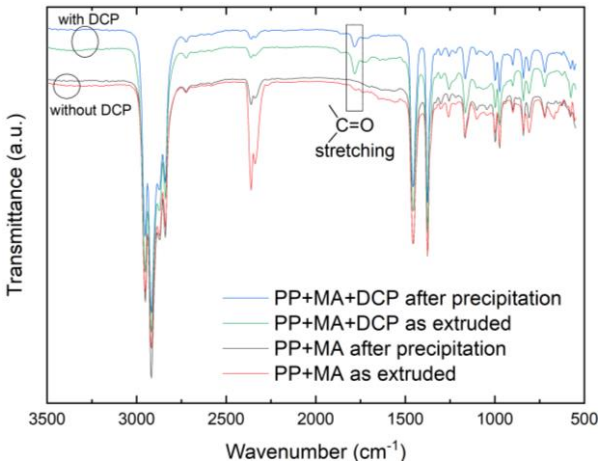

Figure 2: FT-IR spectra of functionalized PP. The C=O absorbance band is highlighted at 1785 cm^{-1}. Extrusion performed without a free radical initiator DCP does not yield covalent attachment between MA and PP. Hence, free MA readily dissolves in acetone during precipitation, and the corresponding C=O stretching band disappears. While reactive extrusion done with DCP, MA is covalently bonded onto PP, and the C=O stretching band is retained after precipitation.

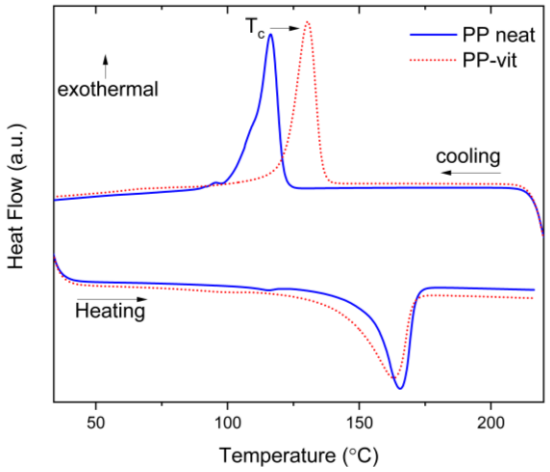

Figure 3: DSC thermogram of vitrimer and its thermoplastic PP precursor. Melting (T_m) and crystallization (T_c) transitions are separated by the usual hysteresis.

throughout the experiment. The plastic creep of PP vitrimer was tested at three different temperature (180, 190 and 200 °C). The evolution of strain with time is represented for each network, see Figure 5(b).

Fused filament fabrication (FFF). Filaments with diameters ca. 1.75 mm were extruded from twin-screw compounder after the crosslinking step was completed. To maintain the uniform diameter the extrusion speed was reduced to 40 rpm, whilst the reactive compounding was carried out at 100 rpm. The slow and steady extrusion of the filament ensures the uniform diameter for the whole length of the filament. Fused filament fabrication of the dynamically crosslinked networks was performed in a commercial 3D printer (Hyrel 3D) with print head MK-250, printing head speed 10mm/s, layered height 0.1 mm and 100% infill. FFF extrusion printing was performed with a nozzle with diameter 0.55 mm at 240 °C. A polycarbonate (PC) or PP plate with thickness 5 mm was employed as a print bed, with the bed temperature maintained at room temperature (ca. 25 °C). PP plate as print bed performed better than PC as higher adhesion is observed for PP.

Shape memory. Quantitative estimation of shape fixing, and shape recovery from an intermediate shape to the initial reference shape was conducted through DMA 850 (TA instrument). Dynamically crosslinked filament extruded from the melt compounder was 3D printed (FFF) into a rectangular sample and mounted between the clamps of DMA in tensile mode. The instrument was equilibrated at 210 °C for 15 min before starting the experiment, see Figure 6d. Thermomechanical cycle consisting of four steps was applied to the sample. (1) Deformation: The rectangular strip was deformed with the application of stress (20 kPa) at a constant stress ramp of 20 kPa/min at 210 °C. (2) Cooling/fixing: With the maintained stress of 20 kPa, the sample was cooled below T_c (≈ 70 °C) at a cooling rate of 10 °C/min to record the stretched shape. (3) Unloading: the stress was released to 0 kPa at a rate of 20 kPa/min. This step fixes the specimen to an intermediate shape. Shape fixity (R_f) is calculated at this step. (4) Recovery: The sample was reheated to 210 °C at 10 °C/min and kept isothermally for 5 min to allow it to recover its natural shape prescribed by crosslinking, before starting the next cycle. Recovery (R_r) of the sample from the intermediate shape to the initial reference shape is calculated after this step. This thermomechanical cycle was repeated several times to evaluate the quality and reproducibility of the shape fixing and recovery. Physical demonstration of shape memory effect was performed on 3D printed rectangular specimen of dimensions 28 mm × 5 mm × 1 mm. The strip was deformed into a twisted shape at 210 °C and cooled (T ≈ 50 °C) under the maintained stress to fix the intermediate shape. The twisted specimen was unloaded. A stress-free reheating of specimen leads to the recovery of the initial shape (see the videos in Supporting Information).

RESULTS AND DISCUSSION

Reactive extrusion of dynamic network

Polyolefins made of solely carbon-carbon and carbon-hydrogen bonds were chosen as a model system to introduce chemical functionality for the dynamic network. Commercial PP with a moderate melt flow index of 34 g/10 min was our base material. Functionalization through solution chemistry was avoided as PP has very limited solubility in common organic solvents. Moreover, a solvent-free chemical functionalization is highly desirable in an industrial setting.[33] Free radical coupling of maleic anhydride initiated by DCP was adopted to introduce anhydride units in the polymer backbone, producing MA-*g*-PP.[14, 34] A lab scale polymer

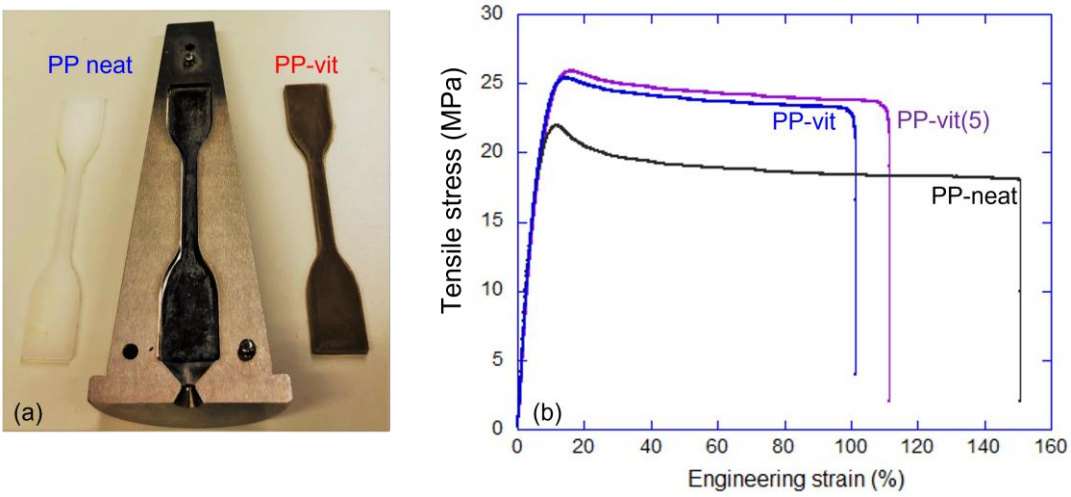

Figure 4. Mechanical properties of PP-vitrimer. (a) ASTM D638 injection mould of the neat PP thermoplastic and the PP-vit, and (b) Stress-strain behaviour of the dynamic vitrimer network (two variants: freshly crosslinked, and after 5 cycles of recycling), and its thermoplastic PP precursor. Tensile strength and extension were measured at room temperature with a crosshead speed of 5 mm/min as in the test specification.

compounder was employed for the reactive extrusion. Radical coupling was performed under constant N_2 flow to maintain inert atmosphere minimizing radical loss. MA-*g*-PP was subsequently crosslinked with chemical moiety bearing bi-functional epoxy groups, PBAEG and catalyst $Zn(acac)_2$ (cf. Figure 1). The efficiency of MA grafting onto PP was confirmed by FT-IR testing, presented in Figure 2. DCP, a free-radical initiator is needed for MA-grafting onto PP. This was proved by a comparison of reactive extrusion of PP with and without the DCP initiator (in the latter case, no MA grafting would occur). After the PP was extruded, it was dissolved in hot xylene and then precipitated in acetone. The FT-IR absorbance band at 1785 cm^{-1} is attributed to the C=O symmetrical stretching. Extrusion of PP and MA without free radical initiator shows very little absorbance at 1785 cm^{-1} from MA, which disappears altogether after precipitation in acetone, as the free MA readily dissolves in acetone and does not precipitate. When reactive extrusion done in presence of DCP, MA is covalently bonded onto PP, hence, even after precipitation in acetone the absorption band corresponding to the C=O bond is retained. Titration method was adopted to quantitively assess the grafting reaction, estimating the fraction of MA grafting as 2.2 wt%.

Epoxy-anhydride curing is believed to undergo via anionic ring-opening copolymerization between epoxy and anhydride.[35, 36] Permanent nature of the crosslinking in vitrimer (PP-vit) was proved by the swelling (gel-fraction) experiment. After immersing in the 'good' solvent - xylene at high temperature (120 °C), an insoluble fraction is recovered. Gel fraction was estimated ≈ 52%. In stark contrast, the thermoplastic precursor PP dissolved in hot xylene within 15 min of immersion. The extent of crosslinking primarily depends on degree of random grafting of MA and the efficiency of anhydride-epoxy curing. In our case, we achieved the gel fraction higher than recently reported literature in polyolefin based vitrimer with different bond exchange mechanism[14].

Melting and crystallization behavior of crosslinked network was probed through DSC. Crosslinking primarily happens in the amorphous segment of the semicrystalline polymer and hence, the overall DSC thermogram would not significantly alter.[30] The heterogeneous microdomain of crosslinked part act as nucleating agent and increases the crystallization temperature (see Figure 3). Crosslinking also acts as physical barrier to segmental mobility and chain packing reducing the overall crystallinity. The heat of fusion was calculated form the area under the endothermic curve of the second heating scan in the DSC profile. We found that the crystallinity fraction was reduced by only 3% in the crosslinked network compared to the thermoplastic precursor. Overall, the semicrystalline nature of the precursor thermoplastic was well preserved upon crosslinking. Moreover, a room-temperature stress-strain behavior (see Figure 4) reveals the improvement of tensile strength. The extruded material was grounded and injection-molded to make samples according to the ASTM D638 standard (see Figure 4a). Compared to the thermoplastic precursor, a slight decrease in the elongation to break is normally observed in vitrimers as the crosslinks act as barrier in chain extension (Figure 4b). This is an insignificant matter since the ductility of over 100% is still observed. The comparison of the precursor PP and its vitrimer, crosslinked at quite a low density, indicates that they have approximately the same linear (Young) modulus: E=380 MPa, determined by the same polycrystalline microstructure, a slightly higher yield stress (no doubt due to added crosslinking): 25-26 MPa vs. 22-23 MPa in the original PP, at about the same tensile strain of 16-18%. The two tensile curves in Figure 4b represent the just-produced vitrimer, and the vitrimer that has been 'recycled' 5 times (chopping into small pieces, re-compounding, and injection molding again). We see no degradation of material properties, which is a positive factor promising true multi-use of this plastic.

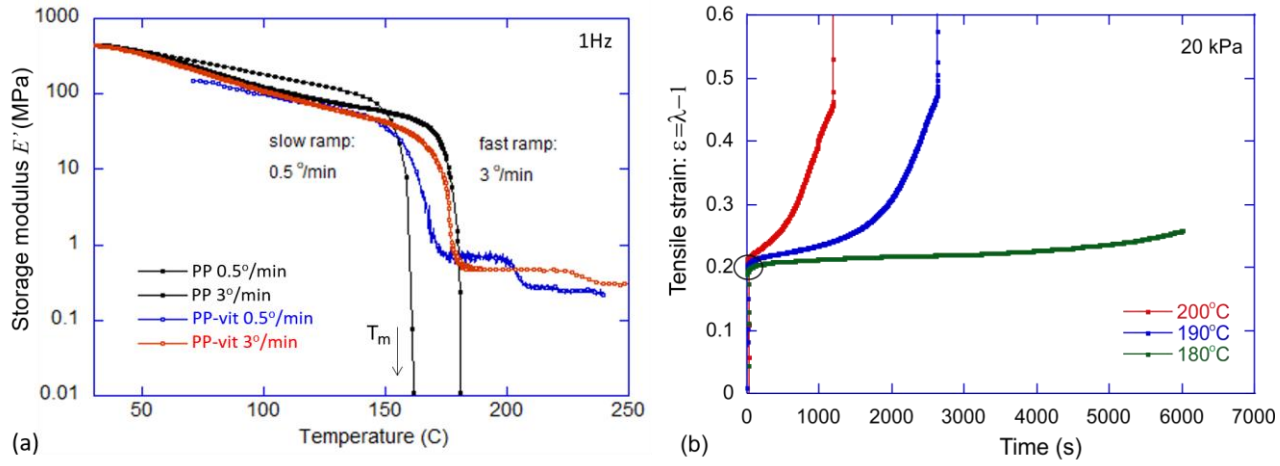

Figure 5. Dynamic mechanical analysis of PP-vit and PP. (a) Evolution of the linear dynamic modulus *E'* of PP-vit and their original PP thermoplastic with temperature. Slower heating rate (0.5 °C min^{-1}) shows the equilibrium melting temperature which matches the one obtained by DSC. (b) 'Iso-stress' creep of the dynamically crosslinked network. An instantaneous tensile stress of 20 kPa is applied on rectangular specimen at the equilibrated temperature in the rubber regime. At higher temperature, bond exchange rate is faster, leading to enhanced creep rate, and hence, the early break. At 180 °C the material responds rubber-elastically, showing very little creep for at least an hour.

Thermo-mechanical properties

Thermomechanical properties of the vitrimer and the thermoplastic precursor were investigated through dynamic mechanical analysis (DMA). Temperature-dependent linear storage modulus (E') is shown in Figure 5(a). The DMA profile of the samples resembles the typical thermoplastic behavior. At lower temperature ($T<T_m$) the storage modulus E' is dictated by the semi-crystallinity. Since the vitrimer retains the overall semi-crystallinity of PP, the modulus is very close to the precursor thermoplastic, until the melting point is reached (which depends on the rate of heating, as indicated in the plot). Beyond the T_m, thermoplastic flows as a viscous liquid. It is also worth to note that the quazi-equilibrium melting temperature obtained at 0.5°/min is more accurately captured in lower heating rate in DMA. In stark contrast, the corresponding dynamically crosslinked network has a non-vanishing E' beyond the T_m, with a signature 'rubber plateau' the hallmark of elastomeric network. PP-vit showed rubber modulus ≈500 kPa and it fairly remained constant till 220 °C. An important feature of the 'rubber plateau' in vitrimers is showing as a step drop: at a higher temperature for a higher heating rate. Although one cannot see the true elastic-plastic transition in a dynamic oscillation test (even at a relatively low frequency of 1 Hz), the onset of rapid bond exchange above the 'vitrification temperature' is reflected in this step drop in the dynamic modulus in Figure 5(a).

Unlike in traditional thermosets, the key characteristics of vitrimer is their ability to plastically flow when heated. The rate of bond exchange reaction underpinning the plastic flow increases with temperature. This is demonstrated by 'iso-stress' creep experiment in DMA presented in Figure 5(b). The sample was equilibrated at a specific chosen temperature, where the bond exchange is sufficiently activated, and an instantaneous stress was applied. This results in an initial elastic response, determined by the rubber modulus, after which a plastic flow (creep) sets in, until the sample finally breaks. At higher temperatures, the measured rate of plastic flow is higher, the enhancement rendered by higher rate of bond reshuffling. Despite permanently crosslinked, the ability of vitrimers to plastically flow under stress opens the possibility of topological reconfiguration through compression molding, injection molding and additive manufacturing. The activation energy of transesterification bond exchange[10] was found to be higher than most other known bond exchanges in vitrimer[14, 37], which makes our dynamically crosslinked network a good choice for applications where creep at service temperature and beyond is not desired.[10] Vitrimers with a lower activation energy undergo significant creep at the vicinity and beyond the melting transitions, diminishing their practical relevance.

Melt flow index (MFI) is an essential parameter to determine processing conditions of plastics. Clearly, our vitrimers are processable, as they are extruded and injection-molded. We measured the MFI of our vitrimers, using the ASTM D1238 process and the standard PP parameters. This gave the MFI =8-10 g/10 min (compared to MFI =34 g/10 min of the original PP), and recalculating the effective viscosity at 230 °C we obtain $\eta = 3 \cdot 10^{-9}$ Pa.s.

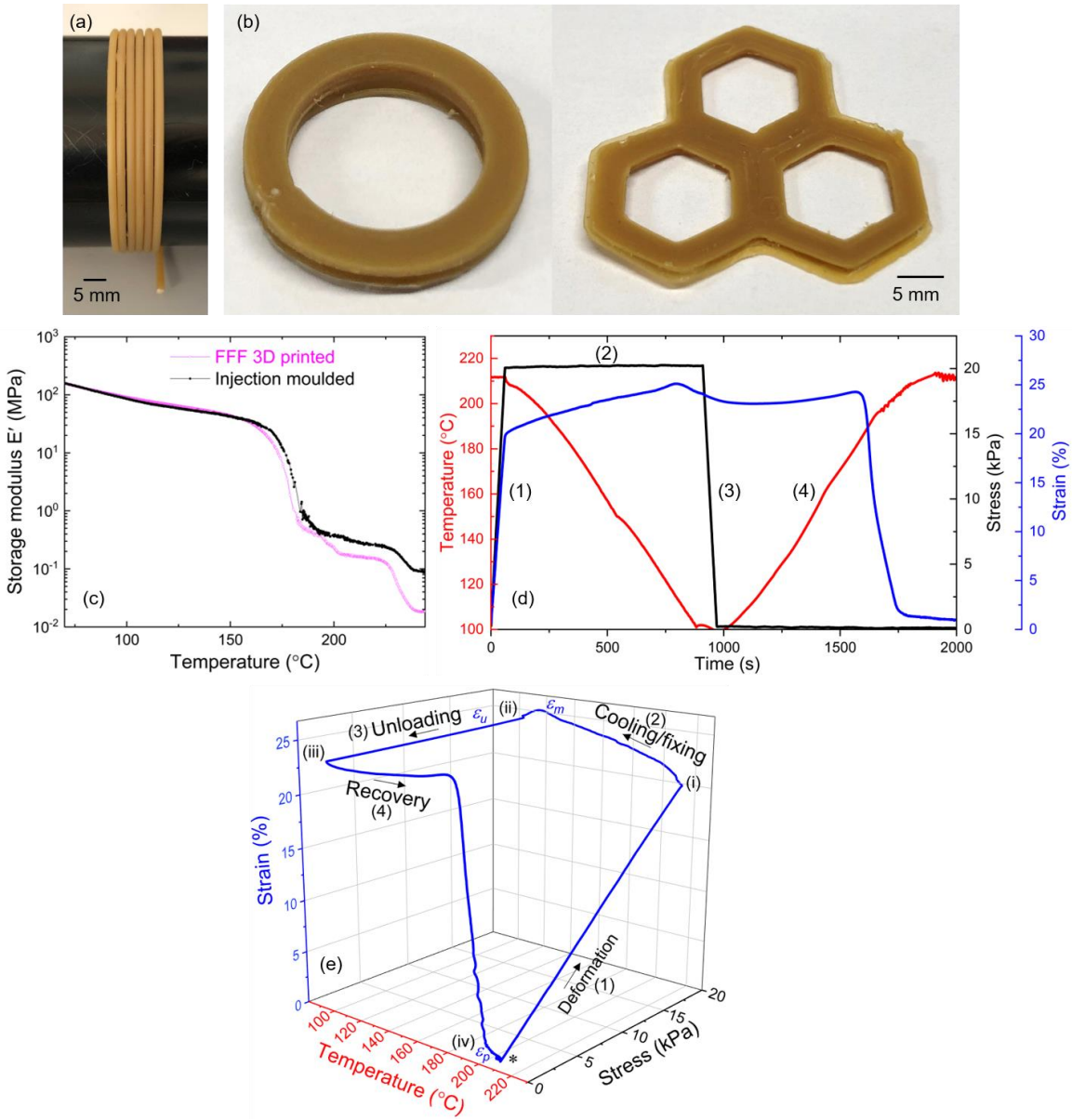

Figure 6. Fused filament fabrication of dynamically crosslinked network, and shape memory. (a) Filament of PP-vit with diameter D ≈ 1.75 mm derived from reactive extrusion, (b) various 3D printed objects, and (c) comparison of storage modulus of injection moulded and 3D printed objects, the slightly lower 'rubber plateau' and the deeper drop of the elastic-plastic transition are explained by the heterogeneous nature of the printed object, made of the thermally extruded filaments. (d) Shape memory in 3D printed dynamically crosslinked network: Thermomechanical cycled conducted in DMA for the estimation of fixity and recovery. (1) Deformation: sample was deformed with a tensile stress (20 kPa) at 210 °C. (2) Cooling/fixing: With the maintained stress of 20 kPa the sample was then cooled below Tc (≈ 70 °C). (3) Unloading: the stress was released to 0 kPa. This step fixes the specimen to a temporal shape. Shape fixity (R_f) is calculated at this step. (4) Recovery: The sample was reheated to 210 °C. (e) Evolution of strain in the PP vitrimer with the application of thermomechanical program demonstrating the fixity-recovery cycle.

Fused filament fabrication of dynamic network

Engineering application can be enormously expanded if fabrication of the smart materials was digitally encoded. With this aim we wanted to explore the fused filament fabrication (FFF method of 3D printing) with the extruded filament of the dynamically crosslinked polymer, see Figure 6(a). The bond exchange reaction above the 'vitrification temperature' enables extrusion via the plastic flow, and the subsequent 3D printing despite the material being permanently crosslinked. As shown in Figure 6(b), objects with various shape were printed in a commercial 3D printer (see Supporting Information movie S1). The evidence of the network integrity after 3D printing is further demonstrated by comparing with DMA profiles of as-extruded specimen with the DMA trace of an original injection-

molded specimen. Figure 6(c) shows that the 3D printed has a slightly lower rubber modulus, and deeper drop at the elastic-plastic transition – but fundamentally the material properties remain the same (especially in the solid plastic state where their main use is expected). In earlier section we have shown that dynamically crosslinked network behaves as a classical SMP, as long as the material is not heated above 'vitrification temperature' under load (in which case the plastic creep would occur).

Enhanced elastic nature of a crosslinked network brings exciting macroscopic properties in response to external stimuli.[38] We now examine the shape memory behavior of the 3D printed objects. Shape memory polymers (SMPs) are a class of solid polymers capable of mechanical programming by a thermal stimulus.[39-41] Broadly, SMPs can 'remember' the one or more reference shapes, determined by the network formation topology, but can be reconfigured to one or more temporary shapes, with the initial reference shape still recoverable. Depending upon the chemical nature of the polymer network the stimulus for recovery could be heat, light. In the present case, the bond exchange reaction is thermally triggered. We found that at load-free reheating, the 3D printed specimen rapidly responds to the thermal stimulus and returns to the reference shape (see Supporting Information movie S2). This further validates the network integrity, and mechanical responsiveness to thermal stimulus is well preserved after fused filament fabrication. The shape-memory response can be quantitatively investigated through a repeated thermomechanical cycle, see Figure 6(d). When SMPs are derived from semicrystalline polymer, as is the case with the PP vitrimer, the material is deformed in the rubbery state above the melting temperature. Subsequently, a programmed shape is fixed through cooling below the crystallization temperature, that immobilizes the polymer chains by arresting the segmental motion. Latent strain energy is stored in this deformed state. The recovery is triggered, through a 'load-free' (with zero applied stress) heating process, by bringing the material back into the rubbery state, when the stored strain energy is released, and the sample returns to the reference shape. The underlying driving force of the recovery is the transition between the network with restricted chain mobility to the state with higher conformational entropy in the rubber-elastic regime. The most important aspect of SMP in practical scenario, and their technological competence, is quantified by measuring the quality of shape fixing (R_f, fixity), and the extent of recovery (R_r, recovery) that can be assessed though DMA thermomechanical cycle shown in Figure 6(d). The extent of shape fixing is calculated as[41],

$$R_f(\%) = \frac{\varepsilon_u}{\varepsilon_m} \times 100,$$

Where, ε_m is the strain achieved after deforming in second step and ε_u is the strain after unloading. The capacity to 'remember' the original shape is determined by extent of recovery. Shape recovery from the programmed shape is obtained though load-free heating. After equilibrating at a high temperature in the rubbery regime, the shape recovery is estimated as[41],

$$R_r(\%) = \frac{\varepsilon_u - \varepsilon_p}{\varepsilon_m - \varepsilon_p} \times 100,$$

where ε_p is the strain achieved after recovery (4th) step, and ε_u and ε_m are same as earlier. From the data plotted in Figure 6(e), these parameters are estimated as: R_f = 92% and R_r = 90%. This high quality of shape fixing, and recovery is making the vitrimer network a good choice for modern technology development with interactive interfaces exploiting the stimuli responsive nature of SMP.

CONCLUSION

Unprecedented usage of non-renewable petrochemical in making plastics leaves a massive carbon footprint. To curb this rising anthropogenic GHG emission it is crucial to consolidate an internal mechanism to recover and upcycle high-value materials from commodity plastics after their service life, thereby minimizing the carbon intensive process of virgin polymer production. We have demonstrated that dynamic covalent chemistry enables thermoplastic materials to turn into high-performance thermosets, retaining mechanical integrity, chemical insolubility, and shape-memory characteristics at service temperature, yet continually re-processable using conventional injection moulding or 3D printing above the 'vitrification temperature'. Although permanently crosslinked, vitrimers undergo creep under stress when the bond exchange is sufficiently activated, giving the underpinning plastic flow. Above the melting transition a classical rubber plateau is identified – a hallmark of elastomeric materials. Fused filament fabrication of these materials was achieved with an excellent dimensional accuracy. The 3D printed specimen not only show mechanical integrity, also high level of responsiveness to thermal stimulus. Thermomechanical cycle employed in dynamic mechanical analysis reveals that shape fixation and shape recovery from the programmed state are well over 90%. Moreover, orthogonality of the bond exchange reaction with a variety of additives and unidentified contaminants makes the near-pristine inputs unnecessary, allowing as-received recycled plastic to be converted to vitrimers. Thus, our work lays a foundation to reclaim megatons of post-consumer thermoplastics, converting them into technically and economically valuable materials.

ASSOCIATED CONTENT

Supporting Information

There are two supporting videos: Fused filament fabrication (3D printing) of dynamically crosslinked network, and Thermally triggered recovery of 3D printed shape memory polymer.

AUTHOR INFORMATION

ORCID
Eugene Michael Terentjev: 0000-0003-3517-6578
Goutam Prasanna Kar: 0000-0003-4290-8765

ACKNOWLEDGEMENTS

This work was supported by the European Research Council AdG No. 786659.

Notes

There are no conflicts to declare.

REFERENCES

1. Geyer, R.; Jambeck, J. R.; Law, K. L., Production, Use, and Fate of All Plastics Ever Made. *Sci. Adv.* **2017,** *3* (7), e1700782.
2. Zheng, J.; Suh, S., Strategies to Reduce the Global Carbon Footprint of Plastics. *Nat. Clim. Change* **2019,** *9* (5), 374-378.
3. Rahimi, A.; García, J. M., Chemical Recycling of Waste Plastics for New Materials Production. *Nat. Rev. Chem* **2017,** *1* (6), 0046.
4. Vollmer, I.; Jenks, M. J. F.; Roelands, M. C. P.; White, R. J.; van Harmelen, T.; de Wild, P.; van der Laan, G. P.; Meirer, F.; Keurentjes, J. T. F.; Weckhuysen, B. M., Beyond Mechanical Recycling: Giving New Life to Plastic Waste. *Angew. Chem. Int. Ed.* **2020,** *59* (36), 15402-15423.
5. Helms, B. A.; Russell, T. P., Reaction: Polymer Chemistries Enabling Cradle-to-Cradle Life Cycles for Plastics. *Chem* **2016,** *1* (6), 816-818.
6. Fortman, D. J.; Brutman, J. P.; De Hoe, G. X.; Snyder, R. L.; Dichtel, W. R.; Hillmyer, M. A., Approaches to Sustainable and Continually Recyclable Cross-Linked Polymers. *ACS Sustain. Chem. Eng.* **2018,** *6* (9), 11145-11159.
7. Van Zee, N. J.; Nicolaÿ, R., Vitrimers: Permanently Crosslinked Polymers with Dynamic Network Topology. *Prog. Polym. Sci.* **2020,** *104*, 101233.
8. Denissen, W.; Winne, J. M.; Du Prez, F. E., Vitrimers: Permanent Organic Networks with Glass-like Fluidity. *Chem. Sci.* **2016,** *7* (1), 30-38.
9. Winne, J. M.; Leibler, L.; Du Prez, F. E., Dynamic Covalent Chemistry in Polymer Networks: a Mechanistic Perspective. *Polym. Chem* **2019,** *10* (45), 6091-6108.
10. Kar, G. P.; Saed, M. O.; Terentjev, E. M., Scalable Upcycling of Thermoplastic Polyolefins into Vitrimers through Transesterification. *J. Mater. Chem. A* **2020,** *8* (45), 24137-24147.
11. Denissen, W.; Rivero, G.; Nicolaÿ, R.; Leibler, L.; Winne, J. M.; Du Prez, F. E., Vinylogous Urethane Vitrimers. *Adv. Funct. Mater.* **2015,** *25* (16), 2451-2457.
12. Lu, Y.-X.; Tournilhac, F.; Leibler, L.; Guan, Z., Making Insoluble Polymer Networks Malleable via Olefin Metathesis. *J. Am. Chem. Soc.* **2012,** *134* (20), 8424-8427.
13. Rekondo, A.; Martin, R.; Ruiz de Luzuriaga, A.; Cabañero, G.; Grande, H. J.; Odriozola, I., Catalyst-free Room-temperature Self-Healing Elastomers based on Aromatic Disulfide Metathesis. *Mater. Horiz* **2014,** *1* (2), 237-240.
14. Röttger, M.; Domenech, T.; van der Weegen, R.; Breuillac, A.; Nicolaÿ, R.; Leibler, L., High-performance Vitrimers from Commodity Thermoplastics through Dioxaborolane Metathesis. *Science* **2017,** *356* (6333), 62-65.
15. Caffy, F.; Nicolaÿ, R., Transformation of Polyethylene into a Vitrimer by Nitroxide Radical Coupling of a Bis-dioxaborolane. *Polym. Chem* **2019,** *10* (23), 3107-3115.
16. Pepels, M.; Filot, I.; Klumperman, B.; Goossens, H., Self-healing Systems based on Disulfide–thiol Exchange Reactions. *Polym. Chem* **2013,** *4* (18), 4955-4965.
17. Obadia, M. M.; Mudraboyina, B. P.; Serghei, A.; Montarnal, D.; Drockenmuller, E., Reprocessing and Recycling of Highly Cross-Linked Ion-Conducting Networks through Transalkylation Exchanges of C–N Bonds. *J. Am. Chem. Soc.* **2015,** *137* (18), 6078-6083.
18. Montarnal, D.; Capelot, M.; Tournilhac, F.; Leibler, L., Silica-Like Malleable Materials from Permanent Organic Networks. *Science* **2011,** *334* (6058), 965-968.
19. Chabert, E.; Vial, J.; Cauchois, J.-P.; Mihaluta, M.; Tournilhac, F., Multiple Welding of Long Fiber Epoxy Vitrimer Composites. *Soft Matter* **2016,** *12* (21), 4838-4845.
20. Zhao, Q.; Zou, W.; Luo, Y.; Xie, T., Shape Memory Polymer Network with Thermally Distinct Elasticity and Plasticity. *Sci. Adv.* **2016,** *2* (1), e1501297.
21. Pei, Z.; Yang, Y.; Chen, Q.; Wei, Y.; Ji, Y., Regional Shape Control of Strategically Assembled Multishape Memory Vitrimers. *Adv. Mater.* **2016,** *28* (1), 156-160.
22. Michal, B. T.; Spencer, E. J.; Rowan, S. J., Stimuli-Responsive Reversible Two-Level Adhesion from a Structurally Dynamic Shape-Memory Polymer. *ACS Appl. Mater. Interfaces* **2016,** *8* (17), 11041-11049.
23. Capelot, M.; Montarnal, D.; Tournilhac, F.; Leibler, L., Metal-Catalyzed Transesterification for Healing and Assembling of Thermosets. *J. Am. Chem. Soc.* **2012,** *134* (18), 7664-7667.
24. Yang, F.; Pan, L.; Ma, Z.; Lou, Y.; Li, Y.; Li, Y., Highly Elastic, Strong, and Reprocessable Cross-linked Polyolefin Elastomers Enabled by Boronic Ester Bonds. *Polym. Chem* **2020,** *11* (19), 3285-3295.
25. Maaz, M.; Riba-Bremerch, A.; Guibert, C.; Van Zee, N. J.; Nicolaÿ, R., Synthesis of Polyethylene Vitrimers in a Single Step: Consequences of Graft Structure, Reactive Extrusion Conditions, and Processing Aids. *Macromolecules* **2021,** *54* (5), 2213-2225.
26. He, Z.; Niu, H.; Liu, L.; Xie, S.; Hua, Z.; Li, Y., Elastomeric Polyolefin Vitrimer: Dynamic Imine Bond Cross-linked Ethylene/Propylene Copolymer. *Polymer* **2021,** *229*, 124015.
27. Saed, M. O.; Lin, X.; Terentjev, E. M., Dynamic Semicrystalline Networks of Polypropylene with Thiol-Anhydride Exchangeable Crosslinks. *ACS Appl. Mater. Interfaces* **2021,** *13* (35), 42044-42051.
28. Spiegel, G.; Paulik, C., Polypropylene Copolymers Designed for Fused Filament Fabrication 3D-Printing. *Macromol. React. Eng.* **2020,** *14* (1), 1900044.
29. Jin, M.; Neuber, C.; Schmidt, H.-W., Tailoring Polypropylene for Extrusion-based Additive Manufacturing. *Addit. Manuf.* **2020,** *33*, 101101.
30. Demongeot, A.; Groote, R.; Goossens, H.; Hoeks, T.; Tournilhac, F.; Leibler, L., Cross-Linking of Poly(butylene terephthalate) by Reactive Extrusion Using Zn(II) Epoxy-Vitrimer Chemistry. *Macromolecules* **2017,** *50* (16), 6117-6127.
31. Schönherr, H.; Wiyatno, W.; Pople, J.; Frank, C. W.; Fuller, G. G.; Gast, A. P.; Waymouth, R. M., Morphology of Thermoplastic Elastomers: Elastomeric Polypropylene. *Macromolecules* **2002,** *35* (7), 2654-2666.
32. Ruiz-Orta, C.; Fernandez-Blazquez, J. P.; Anderson-Wile, A. M.; Coates, G. W.; Alamo, R. G., Isotactic Polypropylene with (3,1) Chain-Walking Defects: Characterization, Crystallization, and Melting Behaviors. *Macromolecules* **2011,** *44* (9), 3436-3451.
33. Moad, G., The Synthesis of Polyolefin Graft Copolymers by Reactive Extrusion. *Prog. Polym. Sci.* **1999,** *24* (1), 81-142.
34. Wang, S.; Ma, S.; Qiu, J.; Tian, A.; Li, Q.; Xu, X.; Wang, B.; Lu, N.; Liu, Y.; Zhu, J., Upcycling of Post-consumer Polyolefin Plastics to Covalent Adaptable Networks via in situ Continuous Extrusion Cross-linking. *Green Chem.* **2021,** *23* (8), 2931-2937.

35. Paul, S.; Zhu, Y.; Romain, C.; Brooks, R.; Saini, P. K.; Williams, C. K., Ring-opening Copolymerization (ROCOP): Synthesis and Properties of Polyesters and Polycarbonates. *Chem. Commun.* **2015,** *51* (30), 6459-6479.
36. Vidil, T.; Tournilhac, F.; Musso, S.; Robisson, A.; Leibler, L., Control of Reactions and Network Structures of Epoxy Thermosets. *Prog. Polym. Sci.* **2016,** *62*, 126-179.
37. Tellers, J.; Pinalli, R.; Soliman, M.; Vachon, J.; Dalcanale, E., Reprocessable Vinylogous Urethane Cross-linked Polyethylene via Reactive Extrusion. *Polym. Chem* **2019,** *10* (40), 5534-5542.
38. McBride, M. K.; Worrell, B. T.; Brown, T.; Cox, L. M.; Sowan, N.; Wang, C.; Podgorski, M.; Martinez, A. M.; Bowman, C. N., Enabling Applications of Covalent Adaptable Networks. *Annu. Rev. Chem. Biomol. Eng.* **2019,** *10* (1), 175-198.
39. Lendlein, A.; Kelch, S., Shape-Memory Polymers. *Angew. Chem. Int. Ed.* **2002,** *41* (12), 2034-2057.
40. Xie, T., Recent Advances in Polymer Shape Memory. *Polymer* **2011,** *52* (22), 4985-5000.
41. Mather, P. T.; Luo, X.; Rousseau, I. A., Shape Memory Polymer Research. *Annu. Rev. Mater. Res.* **2009,** *39* (1), 445-471.